Biomechan Model Mechanobiol
DOI 10.1007/s10237-006-0062-x

ORIGINAL PAPER

Computational modeling of arterial wall growth

Attempts towards patient-specific simulations based on computer tomography

E. Kuhl · R. Maas · G. Himpel · A. Menzel

Received: 23 September 2005 / Accepted: 10 June 2006

Abstract The present manuscript documents our first experiences with a computational model for stress-induced arterial wall growth and in-stent restenosis related to atherosclerosis. The underlying theoretical framework is provided by the kinematics of finite growth combined with open system thermodynamics. The computational simulation is embedded in a finite element approach in which growth is essentially captured by a single scalar-valued growth factor introduced as internal variable on the integration point level. The conceptual simplicity of the model enables its straightforward implementation into standard commercial finite element codes. Qualitative studies of stress-induced changes of the arterial wall thickness in response to balloon angioplasty or stenting are presented to illustrate the features of the suggested growth model. First attempts towards a patient-specific simulation based on realistic artery morphologies generated from computer tomography data are discussed.

Keywords Finite growth · Open system thermodynamics · Stress-induced growth · Restenosis · Patient specific simulation

1 Motivation

Cardiovascular diseases are the most common cause of death in developed nations. Their early diagnosis and qualified treatments are thus of vital importance. A common vascular disease is atherosclerosis, an inflammatory process in which plaque builds up against the inner wall of a large or medium-sized artery. The name atherosclerosis originates from the Greek words athero, meaning gruel or paste and sclerosis, meaning hardness.

Atherosclerosis is a chronic and cumulative complex disease that typically starts in the early childhood and progresses slowly as people grow older. It is believed to be initiated by injuries in the artery wall or more precisely by endothelial dysfunction. Lipids and other transfer products may then diffuse through the injured parts of the arterial wall. A primary mutation of the intima or the endothelium including accumulation of platelets and fibrin increases the proliferation of connective tissue. Further enlargement of the blood pressure is an aftereffect, which in turn stimulates further growth. The dangers related to atherosclerosis are thus twofold: in early stages of the disease, the narrowing of the lumen due to plaque growth is usually compensated by artery enlargement. If the enlargement process is too excessive, the artery eventually bulges on the over-inflated inner tube and forms dangerous net aneurysms.

The second major problem typically occurs at advanced stages of the disease. Vascular smooth muscle cells then migrate, proliferate and synthesize extracellular matrix components on the luminal side of the vessel wall forming a fibrous cap of the atherosclerotic lesion. Inflammatory mediators ultimately induce thinning of this fibrous cap rendering the plaque weak and susceptible to rupture and thrombus formation. The resulting blood clots may significantly narrow the artery and reduce the blood flow through the affected cross

E. Kuhl (✉) · R. Maas · G. Himpel · A. Menzel
Chair of Applied Mechanics, Department of Mechanical and Process Engineering, University of Kaiserslautern,
P.O. Box 3049, 67653 Kaiserslautern, Germany
e-mail: ekuhl@rhrk.uni-kl.de
URL: http://mechanik.mv.uni-kl.de

section or even completely block it. Recent overviews on the medical phenomena associated with atherosclerosis are given e.g. by Shah (1997), Ross (1999), Libby and Aikawa (2002) and Ruggeri (2002), a rather biomechanical characterization is provided by Zohdi et al. (2004, 2005).

Although atherosclerosis has been the subject of intense research for over 100 years, there is still no agent known that successfully reduces plaque growth and gives elasticity back to the vessel walls. It is a common medical treatment to dilate narrowed arteries by a balloon. Unfortunately, typical aftereffects like elastic re-narrowing and other phenomena that re-close the vessel are not unlikely. A major advance in the past decade has been the introduction of the stent. Immediately after stent implantation, endothelial denudation takes place accompanied by the formation of a layer of platelets and fibrin. Activated platelets eject adhesion molecules which attach to leukocytes and begin a process of rolling along the injured artery surface. Growth factors which influence the proliferation and migration of smooth muscle cells from the media into the neo-intima are released from platelets, leukocytes and smooth muscle cells. The resulting neo-intima consists of extracellular matrix of smooth muscle cell and macrophages recruited over several weeks. As time evolves, the increased production of extracellular matrix decreases. At the injured vessel surface, re-endothelialisation might take place. So in-stent restenosis which affects about one-fifth of all patients is largely a result of the formation of neo-intima, see e.g. Zhou et al. (2003).

Atherosclerosis as such is not healable, but may be avoided by prevention. To diagnose and localize atherosclerosis it is important to know the medical history of the individual patient. With the help of computer tomography, it is nowadays possible to visualize the narrowed vessels. Figure 1 shows a typical CT-image from right below the heart. To improve the visibility of the artery a contrast agent was applied before the examination. The CT-images provide two-dimensional information at cutting distances of several millimeters. As such, they can be used to generate individual finite element models for patient-specific simulations. Pioneering steps from traditional empirical to patient-specific finite element-based medical treatment of cardiovascular diseases have been accomplished by Taylor et al. (1998), see also Cipra (2005).

In the present study, balloon angioplasty and stenting of arteries and their aftereffects are considered as examples for stress-induced growth of soft tissues. The growing tissue is modeled within the framework of open system thermodynamics, see Cowin and Hegedus (1976), or Kuhl and Steinmann (2003a), Kuhl et al. (2003) and Kuhl and Balle (2005). This framework is combined with the concept of an incompatible growth configuration, see e.g. Lee (1969) for the original idea in the context of finite plasticity and Rodriguez et al. (1994), Epstein and Maugin (2000) or Garikipati et al. (2004) for its application to finite growth. Here, we closely follow the ideas of Lubarda and Hoger (2002) which were realized computationally in the recent work by Himpel et al. (2005) and Maas (2005). More sophisticated models characterize the growing tissue as a multiphase material. As such they allow for a mass exchange amongst the individual species rather than for a mass exchange with the environment, see e.g. Humphrey and Rajagopal (2002) or Garikipati et al. (2004). Accordingly, they properly account for transport phenomena which are incorporated only phenomenologically through the mass source in the present approach.

In this contribution, focus is placed on the reaction of the artery in response to changes in the mechanical

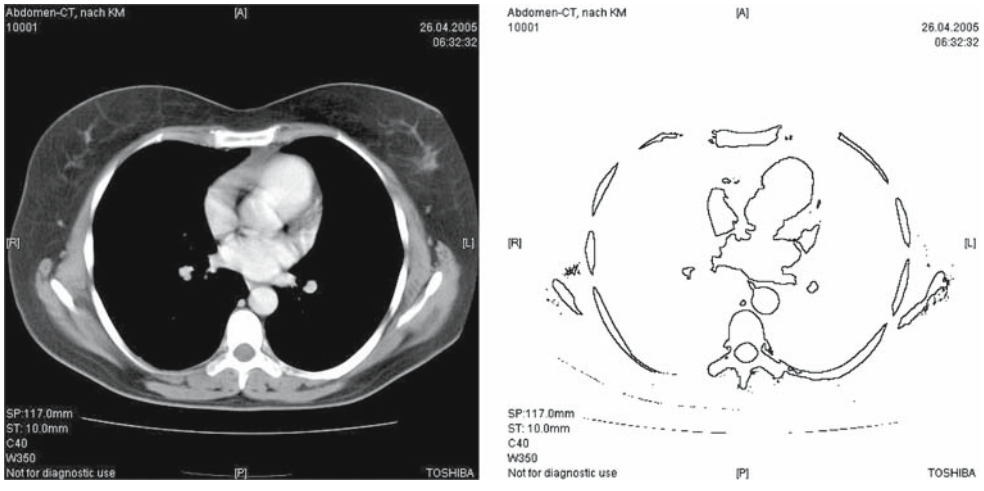

Fig. 1 Human aorta – Typical computer tomography image of characteristic cut and related outline image

loading situation. A direct correlation between the variation in the aortic wall strain and the variation in structural thickness has been reported recently by Blomme et al. (2006). From a microscopic point of view, these thickness changes can be attributed to a variation in the lamellar architecture. In the present approach, however, we shall adopt a macroscopic phenomenological point of view and assume that arterial growth can be characterized through a single scalar valued variable. Enhanced models of anisotropic growth and fiber reorientation have recently been addressed by Kuhl et al. (2005) or Menzel (2005). For the sake of simplicity, the artery is assumed to behave isotropically elastic. More sophisticated constitutive models for arteries can be found in the works of Gasser and Holzapfel (2002), Holzapfel and Ogden (2003) and Holzapfel et al. (2004), Ogden et al. (2005) Balzani et al. (2005). For general overviews of the biomechanics of soft tissues we refer to the excellent monographs by Holzapfel (2000, 2001, 2004), Holzapfel and Ogden (2006), Humphrey (2002) and Humphrey and Delange (2004).

The present manuscript is organized as follows: After a summary of the governing equations based on the concept of open system thermodynamics combined with the kinematics of finite growth in Sect. 2, we briefly sketch the underlying computational realization within a finite element setting in Sect. 3. The basic features of the suggested growth model are then elaborated in Sect. 4. The effects of stent implantation are studied qualitatively, in a healthy and in an atherosclerotic artery. Finally, a first attempt towards a patient-specific simulation based on computer tomography data is illustrated. This work is summarized with an outlook and a final discussion in Sect. 5.

2 Governing equations

To set the stage, we shall briefly introduce the governing equations based on the kinematics of finite growth combined with the framework of open system thermodynamics and supplemented by the corresponding constitutive equations.

2.1 Kinematics of finite growth

Let $\boldsymbol{\varphi}$ denote the deformation mapping particles from a position $\boldsymbol{X}$ in the material configuration $\mathcal{B}_0$ onto a position $\boldsymbol{x} = \boldsymbol{\varphi}(\boldsymbol{X})$ in the spatial configuration $\mathcal{B}_t$. Line elements $\mathrm{d}\boldsymbol{X}$ and $\mathrm{d}\boldsymbol{x} = \boldsymbol{F} \cdot \mathrm{d}\boldsymbol{X}$ of the corresponding tangent spaces $T\mathcal{B}_0$ and $T\mathcal{B}_t$ are then mapped via the deformation gradient $\boldsymbol{F} = \nabla\boldsymbol{\varphi}$. Accordingly, volume elements $\mathrm{d}V_0$ and $\mathrm{d}V_t = J\,\mathrm{d}V_0$ are related via the determinant of the deformation gradient $J = \det(\boldsymbol{F})$. The fundamental assumption of finite growth is the multiplicative decomposition of the deformation gradient $\boldsymbol{F}$ into an elastic part $\boldsymbol{F}_e$ and a growth part $\boldsymbol{F}_g$.

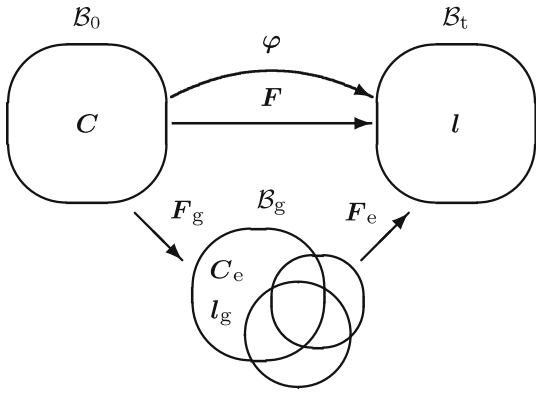

Fig. 2 Kinematics of finite growth — growth tensor

$$\boldsymbol{F} = \boldsymbol{F}_e \cdot \boldsymbol{F}_g \tag{1}$$

In the literature, this multiplicative decomposition and the corresponding introduction of an incompatible growth configuration $\mathcal{B}_g$ dates back to the work of Rodriguez et al. (1994) which was motivated by analogous considerations in finite plasticity, see e.g. Lee (1969) amongst many others. Accordingly, we can then identify the overall right Cauchy Green strain tensor $\boldsymbol{C}$ and its elastic counterpart $\boldsymbol{C}_e$ as relevant deformation measures.

$$\boldsymbol{C} = \boldsymbol{F}^t \cdot \boldsymbol{F} \qquad \boldsymbol{C}_e = \boldsymbol{F}_e^t \cdot \boldsymbol{F}_e \tag{2}$$

Moreover, we introduce the overall velocity gradient $\boldsymbol{l}$ and its growth counterpart $\boldsymbol{l}_g$ as illustrated in Fig. 2.

$$\boldsymbol{l} = \mathrm{D}_t\boldsymbol{F} \cdot \boldsymbol{F}^{-1} \qquad \boldsymbol{l}_g = \mathrm{D}_t\boldsymbol{F}_g \cdot \boldsymbol{F}_g^{-1} \tag{3}$$

Provided that appropriate evolution equations for the growth tensor $\boldsymbol{F}_g$ are given, the above formulation is in principle able to characterize growth of biological tissues. In the simplest form, $\boldsymbol{F}_g$ can be of purely volumetric nature accounting for isotropic growth as

$$\mathrm{d}V_g = J_g\,\mathrm{d}V_0 \tag{4}$$

with the volume elements $\mathrm{d}V_g$ of the incompatible growth configuration $\mathcal{B}_g$ being related to their material counterparts $\mathrm{d}V_0$ through the determinant of the growth tensor $J_g = \det(\boldsymbol{F}_g)$. However, from a biomedical point of view, the above-introduced kinematic growth alone does not seem very reasonable. It obviously implies that

the density of the newly grown material $\rho_g = \rho_0 / J_g$ is now no longer identical to the density ρ_0 of the initial tissue. In order to account for density changes independent from the growth tensor, the kinematical framework of finite growth will be embedded in the framework of open system thermodynamics as illustrated in the following subsection.

2.2 Open system thermodynamics

It is obvious that by growing new material the overall mass of the tissue has to change if the density of the newly added tissue is required to be identical to the one of the original substrate. In order to ensure this density conservation, the balance of mass has to be supplemented by additional terms. Cell migration can be incorporated phenomenologically through an additional mass flux $\boldsymbol{R}$. Moreover, with the help of an additional mass source $\mathcal{R}_0$, phenomena such as increased cell growth, cell division or cell enlargement can be incorporated in order to account e.g. for neo-intima formation in relation with in-stent restenosis. Conceptually speaking, we allow for density changes in the reference configuration in the form of $\rho_0 = \rho_0^* + \int_0^t [\mathrm{Div}(\boldsymbol{R}) + \mathcal{R}_0]\, \mathrm{d}\tau$ where ρ_0^* denotes the initial density prior to growth and ρ_0 now characterizes the density of the tissue after the apposition of new mass as e.g. in Lubarda and Hoger (2002) or Himpel et al. (2005), see Fig. 3. Based on the above considerations, the balance of mass of open system thermodynamics can be expressed as

$$\mathrm{D}_t \rho_0 = \mathrm{Div}(\boldsymbol{R}) + \mathcal{R}_0 \tag{5}$$

see e.g. Cowin and Hegedus (1976) or Kuhl and Steinmann (2003a). Obviously, the newly added mass induces additional momentum, moment of momentum, energy and entropy into the system. Thus, the related higher order balance equations have to be modified accordingly. For example, the volume-specific balance of momentum of open system thermodynamics takes the following format,

$$\mathrm{D}_t(\rho_0 \boldsymbol{v}) = \mathrm{Div}(\boldsymbol{F} \cdot \boldsymbol{S} + \boldsymbol{v} \otimes \boldsymbol{R}) + \boldsymbol{b}_0 + \boldsymbol{v}\,\mathcal{R}_0 - \nabla \boldsymbol{v} \cdot \boldsymbol{R} \tag{6}$$

where $\boldsymbol{S}$ denotes the second Piola Kirchhoff stress tensor and $\boldsymbol{v}$ and $\boldsymbol{b}_0$ are the velocity vector and the momentum source or rather external force vector. Fortunately, this rather cumbersome expression can be modified by subtracting a weighted version of the balance of mass (5) $\boldsymbol{v}\,\mathrm{D}_t \rho_0 = \mathrm{Div}(\boldsymbol{v} \otimes \boldsymbol{R}) + \boldsymbol{v}\,\mathcal{R}_0 - \nabla \boldsymbol{v} \cdot \boldsymbol{R}$ to render the mass specific version of the balance of linear momentum

$$\rho_0 \mathrm{D}_t \boldsymbol{v} = \mathrm{Div}(\boldsymbol{F} \cdot \boldsymbol{S}) + \boldsymbol{b}_0 \tag{7}$$

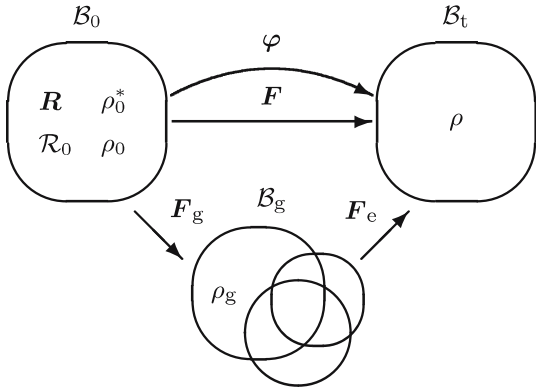

Fig. 3 Open system thermodynamics — mass source and flux

which obviously takes the familiar format known from closed system thermodynamics. Note that similar simplifications can be performed for all the other balance equations such that the open system framework as such poses no additional difficulties, see e.g. Kuhl and Steinmann (2003a). In summary, our formulation allows for change in mass of the form $\mathrm{d}m = \mathrm{d}m^* + [\int_0^t [\mathrm{Div}(\boldsymbol{R}) + \mathcal{R}_0]\, \mathrm{d}\tau]\, \mathrm{d}V_0$, where $\mathrm{d}m^* = \rho_0^*\, \mathrm{d}V_0$ and $\mathrm{d}m = \rho_0\, \mathrm{d}V_0 = \rho_g\, \mathrm{d}V_g$ denote the mass prior to and after growth, respectively. Thus, mass changes can either result from changes in volume captured through the growth tensor $\boldsymbol{F}_g$ or rather its determinant J_g or from changes in density represented though the mass flux and source $\boldsymbol{R}$ and $\mathcal{R}_0$. Accordingly, two special cases can be identified, pure density growth at constant volume with $\mathrm{d}V_g = \mathrm{d}V_0 = \text{const}$ and pure volume growth at constant density with $\rho_g = \rho_0^* = \text{const}$. In the former case, a mass flux and mass source have to be specified constitutively while the growth tensor remains constant. In the latter case which seems reasonable in the context of in-stent restenosis, we have to specify appropriate evolution laws for the growth tensor while the mass source follows accordingly provided that a mass flux is negligibly small. In the following subsection, we shall close the set of governing equations, by specifying the set of constitutive equations. To this end, we suggest to elaborate the reduced dissipation inequality of open system thermodynamics.

$$\begin{aligned} \mathcal{D}_0^{\mathrm{red}} = {} & [\boldsymbol{C}_e \cdot \boldsymbol{S}_e] : [\mathrm{D}_t \boldsymbol{F}_g \cdot \boldsymbol{F}_g^{-1}] \\ & - \rho_0 \mathrm{d}_{\rho_0} \psi [\mathrm{Div}(\boldsymbol{R}) + \mathcal{R}_l] + \mathcal{D}_0^{\mathrm{ext}} \geq 0 \end{aligned} \tag{8}$$

Note that the extra dissipation term $\mathcal{D}_0^{\mathrm{ext}}$ has been introduced in order to satisfy the second law of thermodynamics in the case of arterial wall growth or stiffening, see e.g. Kuhl and Steinmann (2003a,b) or Himpel et al. (2005).

2.3 Constitutive equations

The free energy density of the tissue can be expressed in terms of the overall deformation gradient $\boldsymbol{F}$, the growth tensor $\boldsymbol{F}_{\mathrm{g}}$ and the density ρ_0 as $\psi = \psi(\boldsymbol{F}, \boldsymbol{F}_{\mathrm{g}}, \rho_0)$. However, it proves convenient to reformulate the free energy density in terms of the first and third invariant of the elastic right Cauchy Green tensor $I_1 = \mathrm{tr}(\boldsymbol{C}_{\mathrm{e}})$ and $I_3 = \det(\boldsymbol{C}_{\mathrm{e}})$ as

$$\psi = \tfrac{1}{8}\,\lambda \ln^2(I_3) + \tfrac{1}{2}\,\mu\,[I_1 - 3 - \ln(I_3)] \tag{9}$$

Herein, λ and μ denote the classical Lamé constants. From the standard argumentation of rational mechanics, the second Piola Kirchhoff stress introduced in Eq. (7) follows as $\boldsymbol{S} = 2\rho_0\,\partial_{\boldsymbol{C}}\psi$. Its push forward to the growth configuration $\boldsymbol{S}_{\mathrm{e}} = \boldsymbol{F}_{\mathrm{g}} \cdot \boldsymbol{S} \cdot \boldsymbol{F}_{\mathrm{g}}^{\mathrm{t}}$ then renders the following useful expression

$$\boldsymbol{S}_{\mathrm{e}} = \mu\,\boldsymbol{I} + [\tfrac{1}{2}\,\lambda \ln(I_3) - \mu]\,\boldsymbol{C}_{\mathrm{e}}^{-1} \tag{10}$$

where $\boldsymbol{I}$ denotes the second order identity. In the context of isotropic growth, the growth tensor can be expressed in terms of a single scalar-valued growth factor ϑ.

$$\boldsymbol{F}_{\mathrm{g}} = \vartheta\,\boldsymbol{I} \tag{11}$$

Due to thermodynamic considerations, see e.g. Lubliner (1990) or Himpel et al. (2005), the evolution of the growth factor is assumed to be driven by the current value of ϑ through a growth function $k_\vartheta(\vartheta)$ and by the trace of the elastic Mandel stress $\boldsymbol{C}_{\mathrm{e}} \cdot \boldsymbol{S}_{\mathrm{e}}$, compare Eq. (8).

$$\mathrm{D}_{\mathrm{t}}\vartheta = k_\vartheta(\vartheta)\ \mathrm{tr}(\boldsymbol{C}_{\mathrm{e}} \cdot \boldsymbol{S}_{\mathrm{e}}) \tag{12}$$

Recall that the trace of the elastic Mandel $\mathrm{tr}(\boldsymbol{C}_{\mathrm{e}} \cdot \boldsymbol{S}_{\mathrm{e}})$ is identical to the trace of the overall Kirchhoff stress $\mathrm{tr}(\boldsymbol{F} \cdot \boldsymbol{S} \cdot \boldsymbol{F}^{\mathrm{t}})$ which is a measure of the current stress acting on the tissue. According to Lubarda and Hoger (2002) the coefficient k_ϑ is defined as

$$k_\vartheta = \begin{cases} k_\vartheta^+ \left[\dfrac{\vartheta^+ - \vartheta}{\vartheta^+ - 1}\right]^{m_\vartheta^+} & \text{for } \mathrm{tr}(\boldsymbol{C}_{\mathrm{e}} \cdot \boldsymbol{S}_{\mathrm{e}}) > 0 \\ k_\vartheta^- \left[\dfrac{\vartheta - \vartheta^-}{1 - \vartheta^-}\right]^{m_\vartheta^-} & \text{for } \mathrm{tr}(\boldsymbol{C}_{\mathrm{e}} \cdot \boldsymbol{S}_{\mathrm{e}}) < 0 \end{cases} \tag{13}$$

to avoid unlimited growth. The parameters $\vartheta^+ > 1$ and $\vartheta^- < 1$ describe the limiting values of the growth factor that can be reached by growth and atrophy, respectively. Furthermore, $k_\vartheta^+, m_\vartheta^+$, and k_ϑ^-, m_ϑ^- are constant material parameters in case of tensions and compression, respectively.

On the microscopic scale, growth phenomena are primarily dominated by cell migration and other transport mechanisms. On the macroscopic scale, however, we shall assume that growth is represented phenomenologically through a mass source $\mathcal{R}_0$ which follows straightforwardly from Eq. (12) by making use of the constant density condition $\rho_{\mathrm{g}} = \rho_0^*$.

$$\mathcal{R}_0 = 3\ \rho_0^*\,\vartheta^2\,\mathrm{D}_{\mathrm{t}}\vartheta \tag{14}$$

Without loss of generality, we shall from now on assume that the mass flux and momentum source are negligibly small.

$$\boldsymbol{R} = \boldsymbol{0} \qquad \boldsymbol{b}_0 = \boldsymbol{0} \tag{15}$$

3 Computational framework

In the present section, we briefly sketch the numerical treatment of the growth equations within a finite element framework. In the context of isotropic growth, it proves convenient to introduce the scalar-valued growth factor ϑ as internal variable on the integration point level. Its evolution is governed by Eq. (12) which is discretized in time with an implicit Euler backward scheme introducing the following discrete residual statement.

$$R_\vartheta = -\vartheta + \vartheta_n + k_\vartheta\ \mathrm{tr}(\boldsymbol{C}_{\mathrm{e}} \cdot \boldsymbol{S}_{\mathrm{e}})\,\Delta t = 0 \tag{16}$$

For the efficient solution of the above equation on the integration point level, we suggest a Newton–Raphson strategy based on the consistent linearization of Eq. (16) in the sense of a truncated Taylor series.

$$R_\vartheta^{k+1} = R_\vartheta^k - [1 - \partial_\vartheta \mathrm{D}_{\mathrm{t}}\vartheta\,\Delta t]\,\Delta\vartheta = 0 \tag{17}$$

The above equation defines the incremental update $\Delta\vartheta$ as

$$\Delta\vartheta = \overline{\partial_\vartheta \mathrm{D}_{\mathrm{t}}\vartheta}^{-1}\,R_\vartheta^k \tag{18}$$

whereby we have introduced the following abbreviation.

$$\overline{\partial_\vartheta \mathrm{D}_{\mathrm{t}}\vartheta} = 1 - [\partial_\vartheta k_\vartheta\ \mathrm{tr}(\boldsymbol{C}_{\mathrm{e}} \cdot \boldsymbol{S}_{\mathrm{e}}) + k_\vartheta\ \partial_\vartheta \mathrm{tr}(\boldsymbol{C}_{\mathrm{e}} \cdot \boldsymbol{S}_{\mathrm{e}})]\Delta t. \tag{19}$$

In each local iteration step, the growth factor is updated as $\vartheta^{k+1} = \vartheta^k + \Delta\vartheta$ until convergence is reached, i.e. the discrete local residual (17) is sufficiently reduced. The elastic growth tangent moduli $\mathbf{C}^{\mathrm{eg}} = 2\,\mathrm{d}_{\boldsymbol{C}_{\mathrm{e}}}\boldsymbol{S}_{\mathrm{e}} = 2\,\partial_{\boldsymbol{C}_{\mathrm{e}}}\boldsymbol{S}_{\mathrm{e}} + 2\,\partial_\vartheta \boldsymbol{S}_{\mathrm{e}} \otimes \partial_{\boldsymbol{C}_{\mathrm{e}}}\vartheta$ of the global Newton iteration can then be calculated as

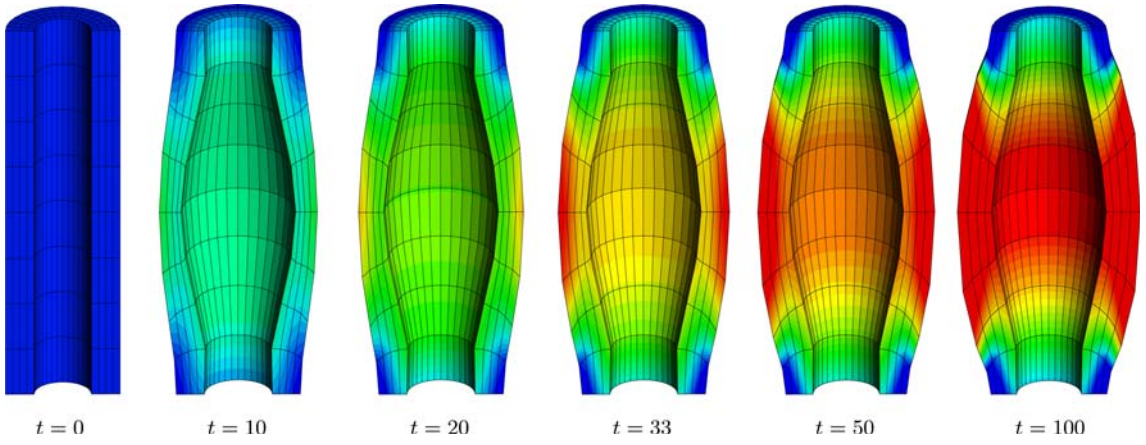

Fig. 4 Qualitative simulation of healthy aorta – aortic growth and evolution of growth factor

$$\mathbf{C}^{\mathrm{eg}} = \mathbf{C}^{\mathrm{e}} - \frac{2}{\vartheta}\,\overline{\partial_\vartheta \mathrm{D}_{\mathrm{t}}\vartheta}^{-1} k_\vartheta\,\Delta t \\ [\mathbf{C}^{\mathrm{e}} : \boldsymbol{C}_{\mathrm{e}}] \otimes \left[\boldsymbol{S}_{\mathrm{e}} + \frac{1}{2}\boldsymbol{C}_{\mathrm{e}} : \mathbf{C}^{\mathrm{e}}\right] \tag{20}$$

in terms of the standard elastic tangent moduli $\mathbf{C}^{\mathrm{e}} = 2\,\partial_{\boldsymbol{C}_{\mathrm{e}}}\boldsymbol{S}_{\mathrm{e}}$ and the abbreviation introduced in Eq. (19). For the linearizations of the individual terms and a detailed description of the algorithmic treatment, we refer to Himpel et al. (2005). Due to the conceptual simplicity of the computational modeling of growth into terms of one single scalar-valued growth factor, the implementation in commercial finite element codes is straightforward. For example, the results presented in the following section are based on simulations with ABAQUS (2005) described in detail by Maas (2005).

4 Examples

In the following section, we shall elaborate the performance of the suggested growth model in the context of arterial wall thickening and stenting of arteries as typical examples of stress-induced growth of soft tissues. The following case studies represent the first stage of our current research project and are thus rather of phenomenological nature. Nevertheless, they provide a first insight into the complex interaction between changes in mechanical loading and tissue growth. Three different cases of increasing complexity are investigated. First, we analyze the behavior of a perfect healthy artery in response to a local increase of the internal pressure. Next, we elaborate the same load case, however, now focussing on the influence of an atherosclerotic plaque. Finally, the suggested growth algorithm is applied to the patient-specific analysis of a human aorta.

4.1 Qualitative simulation of healthy aorta

As a pre-stage to the simulation of a stented aorta, we analyze a cylindrical tube to illustrate the basic features of the proposed model. The elastic material parameters of the tube wall are chosen to $\lambda = 0.577$ N/mm^2 and $\mu = 0.385$ N/mm^2, the growth parameters are taken as $\rho_0^* = 1$ g/cm^3, $\vartheta^+ = 1.3$, $\vartheta^- = 0.5$, $k_\vartheta^+ = 1.0$, $k_\vartheta^- = 2.0$, $m_\vartheta^+ = 2.0$, $m_\vartheta^- = 3.0$ and $\Delta t = 1$, respectively. The set of parameters is adopted from Himpel et al. (2005) where detailed sensitivity studies with respect to different growth parameters can be found. For different identification techniques of the relevant elastic material parameters the reader is referred to Cowin and Humphrey (2001), Holzapfel and Ogden (2003) and Holzapfel and Ogden (2006) and references cited therein. To qualitatively account the mechanical influence of stenting, a smoothly increasing prescribed radial expansion is prescribed in a selected subsection in the middle of the tube. The deformation and the evolution of the growth factor ϑ are illustrated in Fig. 4. A pronounced tissue deposition at areas of increased tension in the middle of the tube can be observed. An artery affected by increased mechanical loading due to stenting or hypertension typically reacts by reinforcing its resistance through increasing its wall thickness. The observed growth phenomena clearly indicate a relation between hypertension and atherosclerosis, especially when taking into account that the realistic elastic boundary conditions in the human body would not allow the artery to bulge out but rather force it to grow to the inside and narrow the lumen. Recall that standard inelastic material

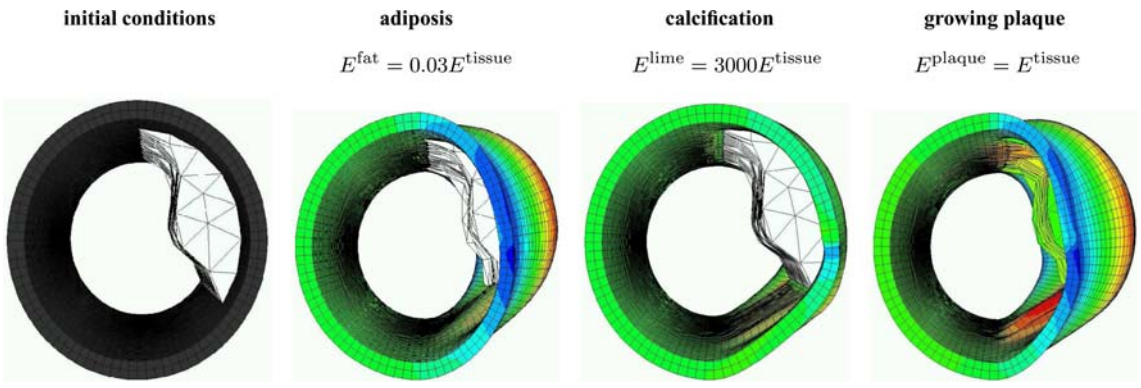

Fig. 5 Qualitative simulation of atherosclerotic aorta — different stages of atherosclerosis: **(a)** initial conditions **(b)** adiposis **(c)** calcification **(d)** growing plaque

models such as damage or plasticity are typically not capable of capturing these effects of volume increase.

4.2 Qualitative simulation of atherosclerotic aorta

Let us now analyze the influence of an atherosclerotic plaque on tissue growth. The initial geometry of the cylindric artery and the plaque is shown in Fig. 5.1. The Lamé constants of the artery are chosen as $\lambda = 1.73077$ and $\mu = 1.15385$. The initial density is $\rho_0^* = 1$ g/cm^3 and the growth parameters take values of $\vartheta^+ = 1.5$, $\vartheta^- + 0.5$, $k_\vartheta^+ = 0.5$, $k_\vartheta^- = 0.25$, $m_\vartheta^+ = 5$ and $m_\vartheta^- = 4$. While the tube has been subjected to prescribed lateral displacements at the inner wall in the previous example, we shall now apply an internal pressure to qualitatively account for stenting.

During atherosclerosis, the atherosclerotic plaque usually undergoes a transition from fatty tissue at an early stage of the disease to a lime-type material at later stages. These, of course, have very different elastic properties. While lime is a very hard and brittle material the fatty tissue is rather soft, even softer than the artery wall itself. To elaborate the different stages of the disease, we thus assign different sets of material properties to the atherosclerotic plaque. In the first example, the plaque is modeled as a soft and fatty tissue with a stiffness of 3% of the wall stiffness. For the calcified state, the plaque is assumed to be 3000 times stiffer than the surrounding artery wall. While in both cases, the plaque is modeled as a non-growing material, not only the artery but also the plaque itself is allowed to grow in a final third case study.

In all three studies, the inner pressure opens the tube pushing the plaque into the artery wall. Close to the atherosclerotic boundary, imperfections cause high stress concentrations on the luminal side of the vessel wall. The different colors in Fig. 5 indicate the values of the growth factor ranging from material resorption of $\vartheta = 0.75$ in the blue areas to material deposition of $\vartheta = 1.25$ in the red domains. As expected, pronounced growth takes place at the boundaries of the plaque in order to compensate local stress concentrations. In the case of adiposis illustrated in Fig. 5b, the applied pressure directly affects the artery wall and thus causes extensive deposition of new material. While the lumen of the artery is almost unaffected by the soft and fatty plaque in Fig. 5b, first effects of cross section narrowing can be observed for the stiff calcified plaque in Fig. 5c For the calcified state depicted Fig. 5c, the overall deformation is not as high as in the first example since, as a matter of course, the stiffer plaque tends to strengthen the artery wall. Accordingly, wall stresses are reduced beyond the plaque. However, high local stress concentrations can be observed at the plaque boundaries causing pronounced local growth in very small areas. These are the areas of potential plaque rupture.

For the sake of comparison, the plaque is finally modeled as a growing material possessing the same growth parameters as the surrounding artery. Recall that for more realistic simulations, growth of the atherosclerotic lesion should be modeled through a mass flux rather than a mass source term. More sophisticated multiphase models, e.g. the ones by Humphrey and Rajagopal (2002) or by Garikipati et al. (2004) could be consulted in order to define appropriate constitutive equations for the mass flux.

The results of our mass source based simulation are shown in Fig. 5d. They illustrate the qualitative effects of in-stent restenosis. Due to huge local stress concentrations around the plaque, a high, wavy growth pattern develops that re-narrows the cross section of the artery. A zoom in of the final state of computational biological equilibrium is given in Fig. 6. It clearly demonstrates that the growth factor ϑ has increased up to almost 25% in regions of pronounced artery wall thickening. The tendency of growing at areas of high stresses and

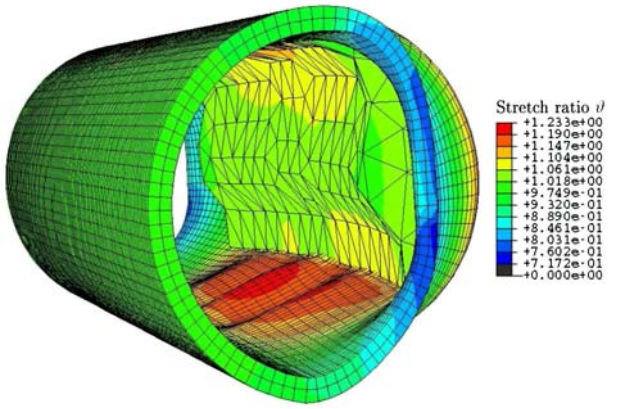

Fig. 6 Qualitative simulation of atherosclerotic aorta — in-stent restenosis and cross section re-narrowing

the possible danger of cross section re-narrowing agrees nicely with the observed phenomena of in-stent restenosis. Especially at the inside wall beyond the area of the plaque, pronounced material ingrowth is observable indicating that re-closure effects are not unlikely.

Comparing the three simulated cases for different plaque compositions, we observe the largest local stress concentrations for the calcified plaque, whereas the stresses are rather uncritical and smooth for the soft and fatty tissue. Since adiposis represents an early state of atherosclerosis, a surgical treatment is often not yet necessary. Besides the danger of narrowing the artery lumen, the fatty plaque as such is not really dangerous. The circulation system is able to compensate the narrowing in most cases by increasing physical activity and changing the pattern of life. The simulation shows that in case of adiposis, the human body may even be able to heal itself under special conditions. The final simulation with the growing plaque nicely documents that the incorporation of growth factors is of cardinal importance, especially if interest is focussed on a changing loading situation. Although being of rather phenomenological nature and not yet fully developed to simulate real biological tissues, the suggested model has been shown capable of identifying regions of local stress concentrations indicating the potential danger of plaque rupture. Moreover, the computational simulation is able to qualitatively predict restenosis effects of re-narrowing of cross sections in response to artery stenting.

4.3 Patient specific simulation of the human aorta

The long-term goal of this project is to provide patient-specific predictions of individual arteries in response to medical surgery. To investigate the features of the suggested growth model, we analyze a real human aorta based on computer tomography data. The CT-data used in the present study contains cross sections of a human abdomen from slightly underneath the heart ranging down to the legs whereby a cutting distance of 10 mm was chosen. Before the examination, a contrast agent was applied to improve the visibility of the artery.

For the generation of a patient-specific geometric model of the aorta the individual CT-images have to be inverted and edited until only the outlines of the required features are visible. The outlined images as depicted in Fig. 1, right, can then be converted into two-dimensional point coordinates, e.g. by a simple MATLAB subroutine which basically generates a three-dimensional data set of point clouds from the two-dimensional outlines of the individual cuts. The spline curves generated from these points define a the solid model of the aorta as depicted in Fig. 7, left, which, after some postprocessing and smoothing, serves as the input for the finite element program.

The widening of the lumen in response to stent or balloon exposure is simulated qualitatively by the application of a uniform pressure of 10 mbar at the inside of the aorta in a predefined subsection. The stent operation usually takes about half an hour corresponding to a time step of Δt in our simulation. Restenosis effects are typically recognized after several weeks. The post-operative response is thus simulated in 1600 time steps corresponding to a period of approximately 1 month after the operation. During that time, we allow for stress-induced growth of the aortic wall in response to changes in the mechanical loading situation. The evolution of the aortic geometry and the scalar-valued growth factor ϑ is depicted in Fig. 8. The results clearly reflect the expected growth at destinations of high stresses. Because of the non-uniform surface of the aorta wall, there is an extensive growth to one side. Approximately 1 month after the operation, see Fig. 8, right, a state of computational biological equilibrium is reached and no additional growth takes place. At that stage, the aorta has fully adapted to changes in the mechanical loading situation.

The role of mechanical stresses in the artery wall is often discussed as a cause for in-stent restenosis by proliferation of cells. Several studies as for instance Zhou et al. (2003), have shown that the mechanical stress caused by oversized stents is positively correlated with the severity of in-stent restenosis. The appropriate stent size in relation to the vessel geometry can minimize the stresses in the vessel wall and therefore decrease the risk of in-stent restenosis, see e.g. Holzapfel et al. (2005). The improved understanding of the interaction of mechanics and growth is thus of fundamental importance in modern stent technology.

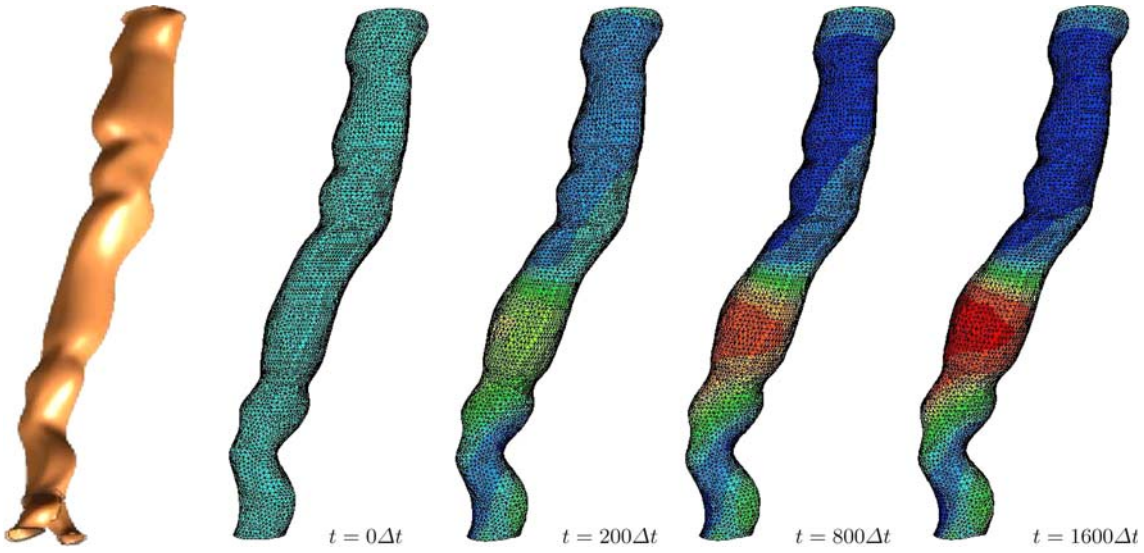

Fig. 7 Patient-specific simulation of the human aorta – aortic growth and evolution of growth factor (lateral view)

Due to the applied, maybe non-physiological boundary conditions, the artery wall grows to the outside. When being embedded into the human body, however, the artery is typically subjected to elastic boundary conditions from the outside. Recent investigations by Blomme et al. (2006) indicate that the boundary conditions, e.g. the additional support introduced by the stiff spine, severely influence the structural development of the artery, even in the healthy state. By incorporating more realistic boundary conditions, the grown material would certainly be pushed to the inside of the artery, perhaps even through the lattice-type stent geometry. The aortic wall thickening predicted by our simulation would then result in the reduction of the lumen according to the phenomena observed in restenosis. The simulation of real atherosclerotic loading and boundary conditions in combination with a discretized stent require the solution of a contact problem exceeding the goals of the present study.

5 Outlook

A model for stress-induced growth in soft biological tissues has been presented. To account for volumetric growth at constant density, the model combines the theories of finite growth and open system thermodynamics. Growth phenomena are captured by a single scalar-valued internal variable which is essentially driven by the Mandel stress. Within a finite element framework, the evolution of this growth factor is evaluated on the integration point level. An implicit Euler backward time stepping scheme is applied to ensure unconditional stability. For the sake of efficiency, the resulting time discrete nonlinear equation for the growth factor is solved iteratively by a local Newton iteration to ensure optimal quadratic convergence. The conceptual simplicity of the proposed model allows for a straightforward implementation of growth on the material subroutine level of commercial finite element codes.

To illustrate the features of the suggested model, qualitative pre-studies of stress-induced changes of the arterial wall in response to stent implantation were presented. Thereby, the complexity of the model was increased successively. After elaborating a healthy artery without imperfections, we focussed on a diseased artery with an atherosclerotic plaque. Different stages of atherosclerosis were simulated by changing the mechanical properties of the plaque. Finally, a first attempt towards the simulation of growth processes in a real human aorta was presented. To this end a patient-specific geometric model of the aorta was generated based on computer tomography data. The results of the simulation convincingly document the potential of the suggested growth model. In principle, the presented approach is able to capture biomechanical phenomena of stress-induced growth such as neo-intima hyperplasia which are very likely to cause in-stent restenosis and cross section re-narrowing.

Nevertheless, it has to be pointed out that the present manuscript only documents our very first attempts in patient-specific simulation. The illustrated analyses have brought up a number of new questions and can by no means be understood as the final solution to the problem. For example, future research certainly has to focus on a more realistic representation of the in vivo

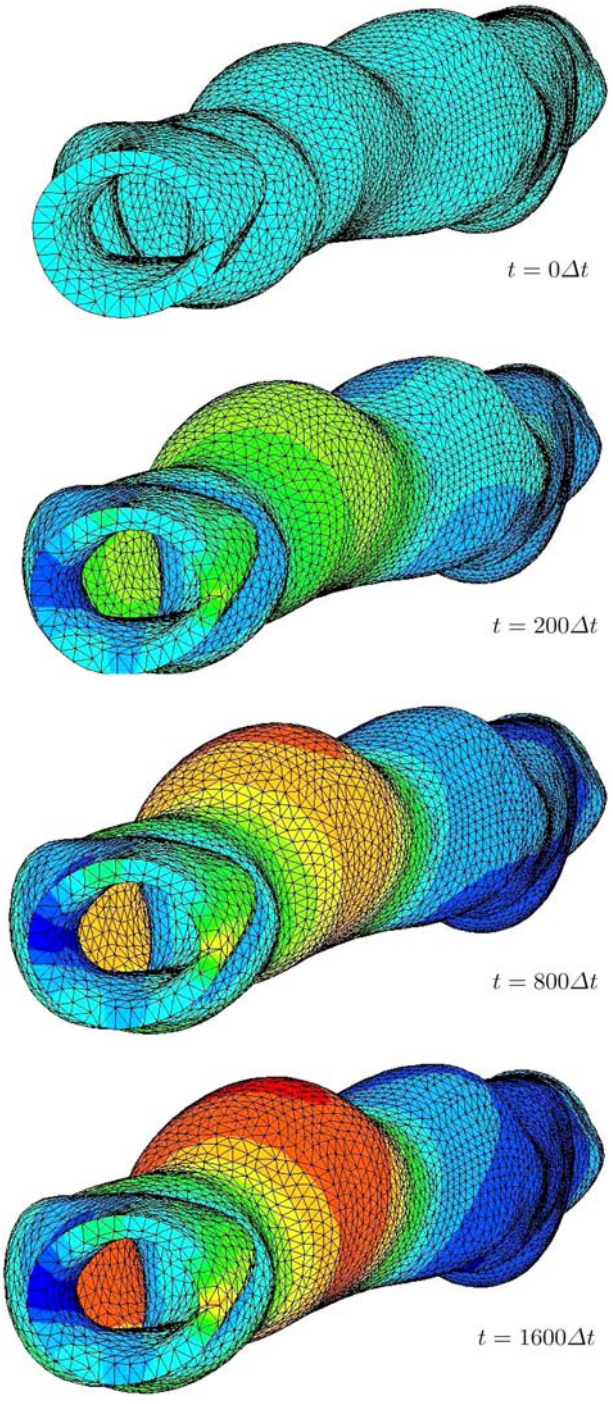

Fig. 8 Patient-specific simulation of the human aorta – aortic growth and evolution growth factor (cross sectional view)

boundary conditions of the artery, which are assumed to largely affect the locations of material apposition in the context of growth. In this context, the influence of the elastic foundation of the artery is currently being elaborated. In addition, it might even become important to include relevant growth factors other then the mechanical stress.

Moreover, more realistic constitutive models for the artery which in reality consists of three mechanically different anisotropic nearly incompressible individual layers have to be adopted. The appropriate simulation of neo-intima formation involves additional numerical complications related to the resolution of the very thin intima layer in comparison to the surrounding media and adventitia. The improvement of the constitutive model for the artery is in line with the identification of patient-specific material parameters. This includes not only the parameters of the growth model but also the elastic material properties of the intima itself which, despite of intensive research, are not yet fully understood.

In the present approach, stenting of arteries has been accounted for exclusively though the boundary conditions. The final goal of this research is, of course, the improvement of stent design supported by the simulation of realistic stents with different geometries. It might even be of interest to simulate the influence of drug-coated stents in the context of diffusion of the growth suppressing substances.

According to the common understanding, plaque vulnerability strongly depends upon the individual tissue morphology. Patient- specific computational simulations are thus of growing interest in modern medical treatment. The ultimate goal of research along these lines is certainly the development of reliable predictive simulation tools that could assist physicians to choose the optimal medical treatment for each individual patient. The present manuscript has shown that patient-specific analyses are in general possible. However, a number of open questions remain providing an open field of potential future research.

Acknowledgments The model of the aorta was created out of computed tomography data and images by courtesy of Dr. med. A. Leppert from the Röntgeninstitut Brandt, Leppert, Rygula und Seybold-Epting, Ärzte für Radiologie und Nuklearmedizin, Kaiserslautern. We gratefully acknowledge their collaboration and friendly support. Moreover, we would like to thank Charles A. Taylor for stimulating discussions on strain-induced growth and remodeling.

References

ABAQUS User's Manual — Version 6.5. (2005) ABAQUS. Inc., USA

Balzani D, Schröder J, Gross D, Neff P (2005) Modeling of anisotropic damage in arterial walls based on polyconvex stored energy functions. In: Owen DRJ, Oñate E (eds), Proceedings of 'COMPLAS 2005'. CIMNE, Barcelona, Spain

Blomme MD, Xu C, Law D, Masuda H, Zarins CK, Taylor CA (2006) Circumferential variation in aortic wall strain and medial lamellar architecture submitted for publication

Cipra BA (2005) Patient-specific models take aim at uncertainty in medical treatment. SIAM News, 38

Cowin SC, Hegedus DH (1976) Bone remodelling I: theory of adaptive elasticity. J Elasticity 6:313–326

Cowin SC, Humphrey JD (2001) Cariovascular Soft Tissue Mechanics. John Wiley, Chichester – New York

Epstein M, Maugin GA(2000) Thermomechanics of volumetric growth in uniform bodies. Int J Plasticity 16:951–978

Garikipati K, Arruda EM, Grosh K, Narayanan H, Calve S(2004) A continuum treatment of growth in biological tissue: The coupling of mass transport and mechanics. J Mech Phys Solids 52:1595–1625

Gasser TC, Holzapfel GA(2002) A rate–independent elastoplastic constitutive model for biological fiber–reinforced composites at finite strains: Continuum basis, algorithmic formulation and finite element implementation. Comp Mech 29:340–360

Himpel G, Kuhl E, Menzel A, Steinmann P (2005) Computational modelling of isotropic multiplicative growth. Comp Mod Eng Sci 8:119–134

Holzapfel GA(2000) Nonlinear solid mechanics: a continuum approach for engineering. John Wiley, New York

Holzapfel GA(2001) Biomechanics of soft tissues. In: Lemaitre J (ed) The handbook of materials behavior models, vol III, Multiphysics Behaviors, Academic, Boston pp 1049–1063

Holzapfel GA(2004) Computational biomechanics of soft biological tissue. In: Stein E, de Borst R, Hughes TJR (eds), Encyclopedia of computational mechanics, vol 2, John Wiley, New York, pp 605–635

Holzapfel GA, Ogden RW(2003) Biomechanics of soft tissue in cardiovascular systems. CISM Courses and Lectures No. 441, Springer, Berlin Heidelberg New York

Holzapfel GA, Ogden RW(2006) Mechanics of biological tissue. Springer, Berlin Heidelberg New York

Holzapfel GA, Gasser TC, Ogden RW(2004) Comparision of a multi-layer structural model for arterial walls with a Fung-type model, and issues of material stability. J Biomech Eng 61:1–48, 2004

Holzapfel GA, Stadler M, Gasser TC(2005) Changes in the mechanical environment of stenotic arteries during interaction with stents: Computational assessment of parameteric stent designs. J Biomech Eng 127:166–180

Humphrey JD(2002) Cardiovasular solid mechanics. Springer, Berlin Heidelberg New York

Humphrey JD, Delange SL(2004) An introduction to biomechanics. Springer, Berlin Heidelberg New York

Humphrey JD, Rajagopal KR(2002) A constrained mixture model for growth and remodeling of soft tissues. Math Models Methods Appl Sci 12:407–430

Kuhl E, Balle F(2005) Computational modeling of hip replacement surgery: Total hip replacement vs. hip resurfacing. Technische Mechanik, 25:107–114

Kuhl E, Garikipati K, Arruda EM, Grosh K(2005) Remodeling of biological tissue: Mechanically induced reorientation of a transversely isotropic chain network. J Mech Phys Solids 53:1552–1573

Kuhl E, Menzel A, Steinmann P(2003) Computational modeling of growth: A critical review, a classification of concepts and two new consistent approaches. Comp Mech 32:71–88

Kuhl E, Steinmann P(2003) Mass– and volume specific views on thermodynamics for open systems. Proc R Soc Lond 459:2547–2568

Kuhl E, Steinmann P(2003) On spatial and material settings of thermo–hyperelastodynamics for open systems. Acta Mech 160:179–217

Lee EH(1969) Elastic-plastic deformation at finite strains. J Appl Mech 36:1–6

Libby P, Aikawa M(2002) Stabilization of atherosclerotic plaques: new mechanisms and clinnical targets. Nat Med 8:1257–1262

Lubarda VA, Hoger A(2002) On the mechanics of solids with a growing mass. Int J Solids Struct 39:4627–4664

Lubliner J(1990) Plasticity Theory. Macmillan Publishing Company, New York

Maas R(2005) Biomechanics of soft tissues. Diploma thesis, LTM, University of Kaiserslautern, U05–01

Menzel A(2005) Modeling of anisotropic growth in biological tissues — a new approach and computational aspects. Biomech Model Mechanobiol 3:147–171

Ogden RW, Saccomandi G, Sgura I(2005) A phenomenological three-dimensional theory of the wormlike chain. Proc R Soc Lond A, (in press)

Rodriguez EK, Hoger A, Mc Culloch AD(1994) Stress-dependent finite growth in soft elastic tissues. J Biomech 27:455–467

Ross R(1999) Atherosclerosis — An inflammatory disease. N Engl J Med 340:115–126

Ruggeri ZM(2002) Platelets in atherothrobosis. Nat Med 8:1227–1234

Shah PK(1997) Plaque disruption and coronary thrombosis: new insight into pathogenesis and prevention. Clin Cardiol 20 (Suppl. II):II–38–II–44

Taylor CA, Hughes TJR, Zarins CK(1998) Finite element modeling of three-dimensional pulsatile flow in the abdominal aorta: relevance to atherosclerosis. Ann Biomed Eng 26:975–987

Zhou R-H, Lee T-S, Tsou TC, Rannou F, Li Y-S, Chien S, Shyy JY-J(2003) Stent implantation activates akt in the vessel wall: role of mechanical stretch in vascular smooth muscle cells. Arterioscler Thromb Vasc Biol 23:2015–2020

Zohdi TI(2005) A simple model for shear stress mediated lumen reduction in blood vessels. Biomech Model Mechanobiol available online first: DOI 10.1007/s10237–004–0059–2, 2005

Zohdi TI, Holzapfel GA, Berger SA(2004) A phenomenological model for atherosclerotic plaque growth and rupture. J Theor Biol 227:437–443